Dielectric Characteristics of Electric Vehicle Traction Motor Winding Insulation under Thermal Ageing

K. N. Gyftakis, *Member, IEEE*, M. Sumislawska, D. F. Kavanagh, D.A Howey, *Member, IEEE* and M. McCulloch, *Senior Member, IEEE*

***Abstract*— The electric motor is the electric vehicle's heart. It is crucial that any occurring faults are detected promptly so that a catastrophic failure is avoided. At the same time, a deep knowledge of the degradation mechanisms is required to allow maximum performance at minimum cost. This paper focuses on this balance. Statistical results from measurements of unaged and accelerated aged winding insulation samples provide information about the degradation processes, enabling steps towards a reliable prognosis model of the motor's remaining life.**

***Index Terms*— Ageing, Dielectric properties, Electric motor, Electric vehicle, Winding Insulation.**

I. Introduction

ELECTRIFIED vehicles are important in addressing the challenges of air pollution and climate change [1]. To increase the uptake of this technology, it is crucial to reduce cost and at the same time increase reliability.

At the heart of the electric vehicle is the electric motor. There are many factors (thermal, electrical, ambient and mechanical, abbreviated TEAM) which influence the degradation and ageing of the motor components or may even cause an unexpected catastrophic failure [2]. When faults appear in electric motors, various methods have been proposed to diagnose the fault, categorize it and in many cases to detect its severity [3]-[5]. Significant work has also been accomplished in the area of prognosis, which is strongly connected with the overall assessment of the motor condition and estimation of remaining life [6]-[8]. However, in order to make machines cheaper, lighter (low carbon) and more reliable it is necessary to understand the degradation mechanisms and consequently design and operate motors closer to their limits.

Research reviews like [3] have shown that, in induction motors most faults occur in the bearings and the winding insulation materials. In both cases there have been some research studies that aimed to understand the physical and chemical properties, which lead to failure, some of which will be highlighted now.

In [9], an investigation using Finite Element Analysis (FEA), Hashin and Shtrikman performed approximation and experimental testing on the thermal properties for both infiltrated and non-infiltrated copper windings. In that case, FEA did not provide satisfactory results. Moreover, there have been numerous contributions dealing with the properties of electrical machine windings [10]-[12]. In [13]-[14] the authors have presented a reliable way to monitor the winding insulation by measuring and analyzing the windings phase currents. Furthermore in [15], the authors applied a Design of Experiments (DOE) approach to define and validate a theoretical life span model. Moreover, twisted pair samples were used in [16] and the authors experienced a decrease of the Partial Discharge Inception Voltage (PDIV) with a simultaneous increase of the turn-to-turn capacitance. Finally, in [17] the thermal modelling of an electrical traction motor was applied for a hybrid drive.

Many different insulation materials (mica, polyamide-imide or PAI, polyester, epoxy etc.) are used in electric machines, each typically serving a different purpose [15]-[18]. Amongst these, PAI is mostly used in the form of an enamel coating on conductor wires which form the machine windings. PAI is chosen because it has good high temperature performance. However, more work needs to be undertaken to investigate the properties of these materials when used as an enamel coating on copper conductor wires [19].

The purpose of this work here is the study of the dielectric properties of PAI insulation material used for coating copper wires. Firstly, measurements on a large population of unaged (i.e. aged at room temperature) samples were taken, since this is crucial for extracting information about manufacturing imperfections of the coating process. Secondly, samples of insulated wire were subjected to accelerated thermal ageing tests in order to study the impact of temperature and ageing time on their dielectric properties, which could be indicative of degradation and failure.

This work is part of the EPSRC funded FUTURE Vehicles project (EP/I038586/1).

K. N. Gyftakis was with University of Oxford and is with Coventry University, UK (email: k.n.gyftakis@ieee.org)

M. Sumislawska is with Coventry University, UK (email: malgorzata.sumislawska@coventry.ac.uk)

D. F. Kavanagh is with Institute of Technology Carlow, Carlow, Ireland (email: darren.kavanagh@itcarlow.ie)

D. A. Howey and M. McCulloch are with University of Oxford, UK ({david.howey, malcolm.mcculloch}@eng.ox.ac.uk)

II. Experimental Setup and Procedure

Firstly, 20 samples were left aside unaged in order to measure and extract baseline information about the expected spread of properties after manufacture. Then, 180 additional samples were divided into 6 groups of 30 samples each. Each group was placed in a separate temperature controlled oven. The 6 ovens were set at 200 °C, 215 °C, 230 °C, 245 °C, 260 °C and 275 °C internal temperature respectively. The ageing time periods were selected to be 100 hrs, 200 hrs, 400 hrs, 800 hrs and 1600 hrs. At the end of each ageing period, 6 samples were removed from the oven. One of the ovens with some samples inside is shown in Fig. 1.

Fig. 1. One of the six identical ovens with samples inside.

For measurement, each sample was placed in a specially fabricated plastic case and its dielectric properties measured with a custom built electrode at 6 different positions, each separated by 3.8 cm, as shown in Fig. 2. The equipment used is the PSM1735 from N4L.

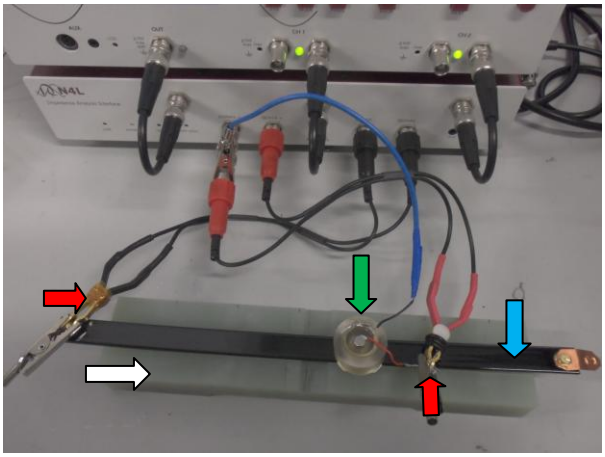

Fig. 2. The measuring bench: white arrow shows the plastic case, blue shows the tested sample, red arrows shows the electrodes (applied voltage) and green shows the prototype moveable electrode.

Table I summarises the number of measurements taken for each case. In some samples the insulation was aged to the point of catastrophic failure and consequently no measurements were taken from these specimens, see (Fig. 3).

TABLE I
Measurements Performed/Expected

	Ageing Period (hours)				
State	**100**	**200**	**400**	**800**	**1600**
unaged	120/120				
200 °C	36/36	36/36	36/36	36/36	36/36
215 °C	36/36	36/36	36/36	36/36	36/36
230 °C	36/36	36/36	36/36	36/36	13/36
245 °C	36/36	36/36	36/36	25/36	0/36
260 °C	36/36	36/36	33/36	4/36	0/36
275 °C	36/36	36/36	7/36	0/36	0/36

Fig. 3. Catastrophic insulation failure of samples at 260°C after 1600 hours.

III. Equivalent Circuit Model

A plot of an example impedance measurement from an insulation sample is presented in Fig 4. The insulation impedance is characterised by capacitive behaviour for frequencies above 1 kHz and mainly resistive behaviour for frequencies below 1 kHz. Therefore, the impedance within the considered frequency range can be modelled using an equivalent circuit model (ECM) comprising a resistor R and capacitor C connected in parallel. The impedance of the considered ECM is given by

$$Z(j\omega) = \frac{R}{RCj\omega+1} \quad (1)$$

where ω is the frequency expressed in radians per second and $j = \sqrt{-1}$.

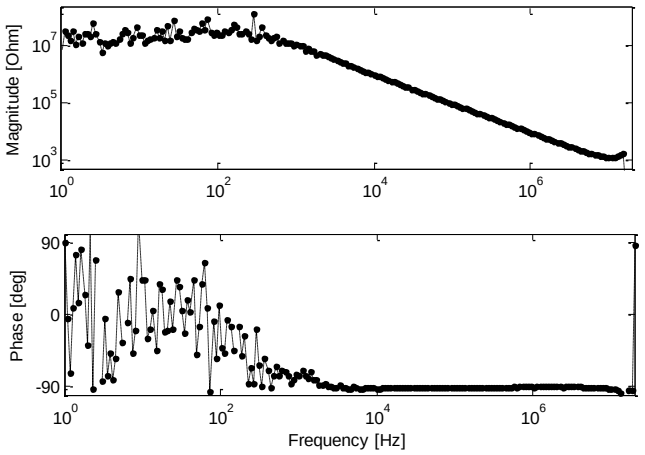

Fig. 4. Impedance spectroscopy of the insulation sample.

A. *Estimation of C*

Note that for $\omega \gg RC$ the impedance of the ECM (1) becomes

$$Z_C = Z(j\omega|\omega \gg RC) \approx \frac{1}{j\omega C} \quad (2)$$

Hence, for $\omega \gg RC$, the magnitude of the impedance is $\frac{1}{\omega C}$, whilst the phase angle is approximately constant and equal to -90 degrees. Thus, the magnitude of the impedance measurement has been used for estimation of *C* in this region. In order to avoid numerical inaccuracies due to round-off errors, the logarithm of the impedance magnitude has been used to calculate *C*, noting that:

$$\log_{10} C = -\log_{10}\omega - \log_{10} Z_C \quad (3)$$

Using the notation $c = \log_{10} C$, the parameter *C* has been estimated as a mean value of $(-\log_{10} 2\pi f - \log_{10} Z_C)$ for 1 kHz < f < 5 MHz [20]. Subsequently, *C* has been calculated as $C = 10^c$.

B. *Estimation of R*

For $\omega \ll RC$ the impedance of the ECM (1) becomes

$$Z(j\omega|\omega \ll RC) \approx R \quad (4)$$

Thus, measurements of the impedance magnitude for f < 100 Hz have been used to estimate the value of *R* [20].

IV. Experimental Results

A. *Unaged Samples Results*

The histogram of estimated values of *C* of unaged samples is presented in the Fig. 5a) The mean is 22.2 pF and the standard deviation is 2.5 pF. Similarly, the histogram of estimates of *R* is presented in the right subfigure of Fig. 5-b. Unlike the high frequency (above 1 kHz) data, the low frequency impedance measurements are strongly affected by measurement noise; in this case the mean was 32.0MΩ and the standard deviation 3.2MΩ. Tables II and III illustrate the samples capacitance and resistance measurements in more detail respectively. Additionally, Fig. 6 illustrates the scatter plot of the measured points' capacitance versus their resistance values.

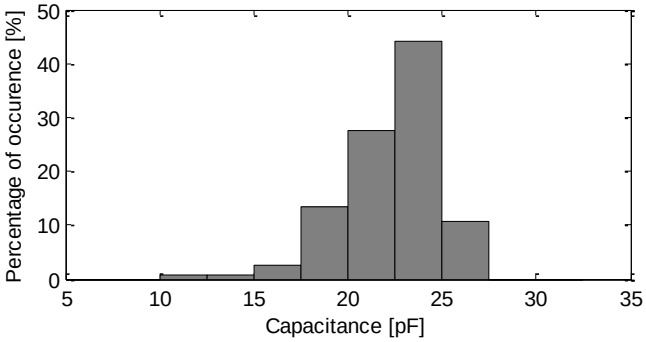

a)

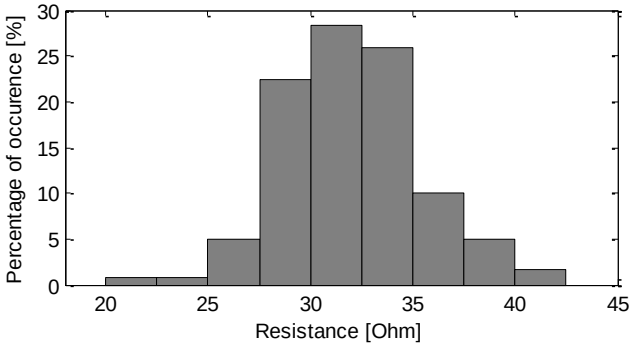

b)

Fig. 5. Histogram of estimated: a) capacitance and b) resistance values from all unaged samples.

TABLE II
SAMPLES CAPACITANCE DISTRIBUTION

Limits [pF]	Number of points	Percentage (%)
10.0 – 12.5	1	0.83
12.5 – 15.0	1	0.83
15.0 – 17.5	3	2.50
17.5 – 20.0	16	13.33
20.0 – 22.5	33	27.50
22.5 – 25.0	53	44.17
25.0 – 27.5	13	10.83

TABLE III
SAMPLES RESISTANCE DISTRIBUTION

Limits [MΩ]	Number of points	Percentage (%)
20.0 – 22.5	1	0.83
22.5 – 25.0	1	0.83
25.0 – 27.5	6	5.00
27.5 – 20.0	27	22.50
30.0 – 32.5	34	28.33
32.5 – 35.0	31	25.83
35.0 – 37.5	12	10.00
37.5 – 40.0	6	5.00
40.0 – 42.5	2	1.67

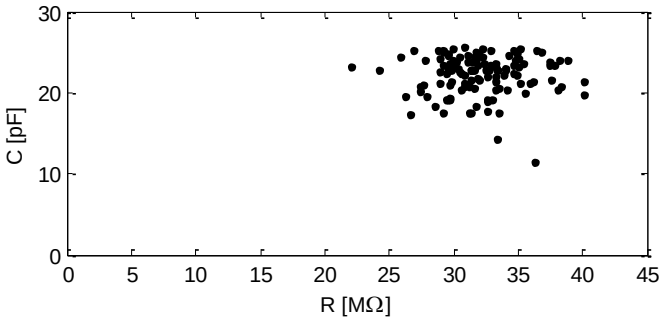

Fig. 6. Scatter plot of the unaged samples measured capacitance versus resistance.

B. *Aged Samples Results*

In the following Fig. 8-Fig. 13 scatter plots of the estimated capacitance and resistance values for the aged samples are presented for each temperature case at various time lengths of exposure. Moreover, Fig. 7 is provided for the reader's convenience, categorizing the samples points' coloured shapes.

Additionally, Tables IV and V present the average values of capacitance and resistance respectively of all measured samples of the same temperature-ageing time group.

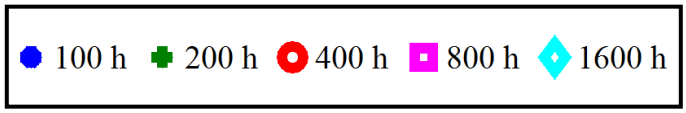

Fig. 7. Classification of the symbolism for Figures 8-13.

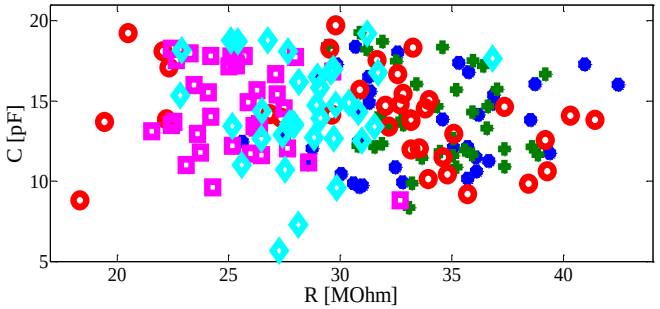

Fig. 8. Scatter plot of the samples measured capacitance versus resistance at 200°C.

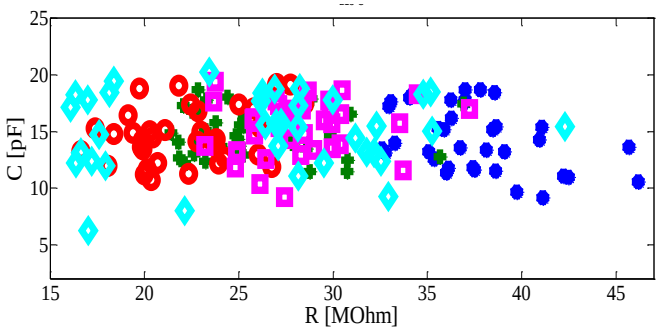

Fig. 9. Scatter plot of the samples measured capacitance versus resistance at 215°C.

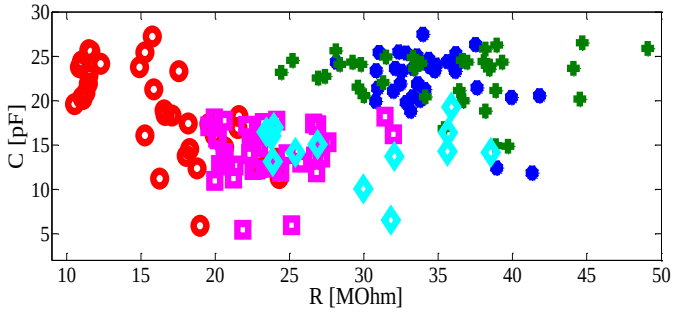

Fig. 10. Scatter plot of the samples measured capacitance versus resistance at 230°C.

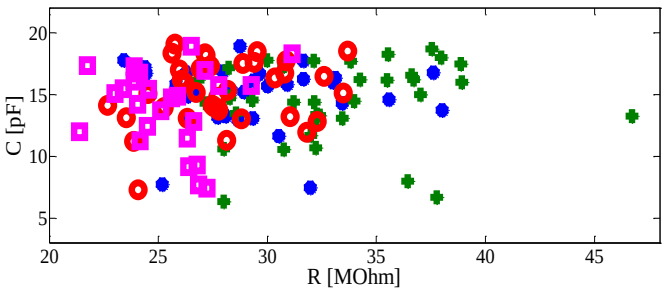

Fig. 11. Scatter plot of the samples measured capacitance versus resistance at 245°C.

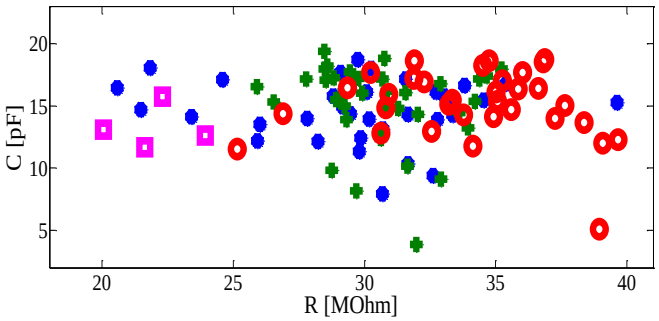

Fig. 12. Scatter plot of the samples measured capacitance versus resistance at 260°C.

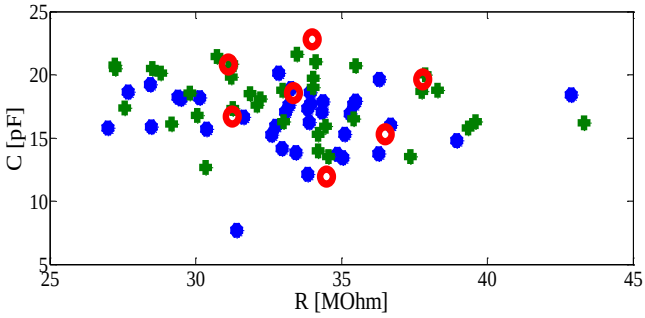

Fig. 13. Scatter plot of the samples measured capacitance versus resistance at 275°C.

TABLE IV
AVERAGE CAPACITANCE (PF) FOR ALL AGED CASES

	100 h	200 h	400 h	800 h	1600 h
200°C	13.6±0.9	14.0±1.0	14.1±0.9	14.5±0.9	14.4±1.1
215°C	14.4±1.0	14.8±0.7	14.7±0.8	15.3±0.8	15.1±1.1
230°C	22.4±1.1	22.7±1.0	18.8±1.7	14.1±1.0	14.3±1.9
245°C	15.1±0.8	14.4±1.1	15.2±0.9	13.0±1.3	----
260°C	14.7±0.8	15.0±1.1	15.1±1.0	13.3±2.8	---
275°C	16.4±0.8	18.0±0.8	17.0±3.4	---	---

TABLE V
AVERAGE RESISTANCE (MΩ) FOR ALL AGED CASES

	100 h	200 h	400 h	800 h	1600 h
200°C	33.5±1.3	34.4±0.8	31.6±2.0	25.4±0.8	28.4±0.9
215°C	37.5±1.1	25.8±1.3	22.2±1.0	28.3±1.0	25.0±2.3
230°C	34.4±1.0	35.1±2.0	16.2±1.4	23.6±1.1	29.0±2.3
245°C	29.0±1.2	33.1±1.5	27.9±1.0	25.5±0.9	---
260°C	29.0±1.4	30.6±0.8	34.1±1.2	21.0±2.5	---
275°C	33.3±1.1	33.2±1.3	34.1±2.3	---	---

C. Discussion on the Experimental Results

Firstly, it is important to note the properties of the unaged samples, whose average capacitance value was about 22 pF. In contrast, the capacitance of the aged samples is less than 20 pF in almost all cases except some measurements on the set aged at 230 °C. This indicates a rapid drop of the capacitance during the early ageing period ($<100hrs$). As a consequence Fig. 6 and Table II reveal that, there exist a serious percentage of weak points of low capacitance, possibly because of the

manufacturing process of the insulation. More specifically, about 17 % of all measurements of the unaged samples present similar capacitance to the aged samples. Amongst them, about 1 % exhibits half the average capacitance value.

The average resistance of the unaged samples was about 32 MΩ. It can be seen that, the resistance is less negatively affected by the manufacturing process compared to the capacitance. That is because the worst case is about 1% of the points, which was characterized by about 2/3 of the average resistance.

It becomes clear that, for proper prognosis of insulation in electric machines, the manufacturing variations and subsequent variation in dielectric properties need to be seriously considered.

Moving on to the aged samples, it can be seen in Fig. 8 that, the capacitance is not practically affected by the ageing temperature. This is also supported by the average values given in Table IV. On the other hand, a gradual decrease of the insulation resistance is observed for the first 800 hrs. After that period the insulation resistance starts increasing again. This is probably due to the air bubbles, which have started to develop together with the chemical change of the insulation material properties.

A similar behavior is noticed for the case of 215 °C (Fig. 9). The main difference here is that the insulation resistance clearly decreases for the first 400 hrs and then it increases again. Despite this, some points aged up to 1600 hrs maintain low resistance values. The capacitance does not seem to be affected by the ageing temperature for this case also.

The samples which were aged at 230 °C are very interesting (Fig. 10). It can be seen that, for the first two ageing period cases, 100 hrs and 200 hrs, the insulation material seems to have statistically the same behavior. Then, when the insulation material ages for 400 hrs there is a distinct decrease in resistance of about 50%. Moreover, a 17 % capacitance (compared with 200 hrs) decrease is observed. When reaching 800 hrs, the material is characterized by a 38% decrease of its capacitance (compared with 200 hrs). At the same time its average resistance starts to increase again (about 46% compared to the samples from 400 hrs). Finally, at 1600 hrs the capacitance remains unchanged with the samples from 800 hrs, but on the other hand the resistance keeps increasing (about 26% compared to the samples from 800 hrs). It is to be noted that, for the case of the samples at 1600 hrs, the average capacitance and resistance are calculated with 13 instead of 32 expected measurements (Table I). It is safe to consider that the dielectric properties of the remaining points, which were actually measured, represent critical insulation material values.

Furthermore, for the case of 245 °C ageing, the capacitance does not vary with ageing time and the resistance presents an initial increase up to 200 hrs and then it progressively decreases again. Unfortunately no samples survived the 1600 hrs ageing process at this temperature.

Additionally, for the last two temperature cases, it becomes clear that the ageing progresses rapidly. Generally both the capacitance and the resistance of the insulation material do not vary much with the ageing time. The only exception is the 30% decrease of resistance from 400 hrs to 800 hrs for the samples at 260 °C, however this result is not reliable since only 4 out of 36 expected measurements were able to be performed (Table I).

Finally, the visual inspection of the tested samples revealed that, there are two different ageing mechanisms depending on the applied temperatures. In the first case, the material ages slowly, bubbles are formed on the surface of the conductor and then the insulation eventually cracks in a zigzag shape (Fig. 14). This was not observed in the samples at 275°C where, the insulation was very rapidly aged and cracked, resulting to local spots of copper bar without any insulation coating (Fig. 15).

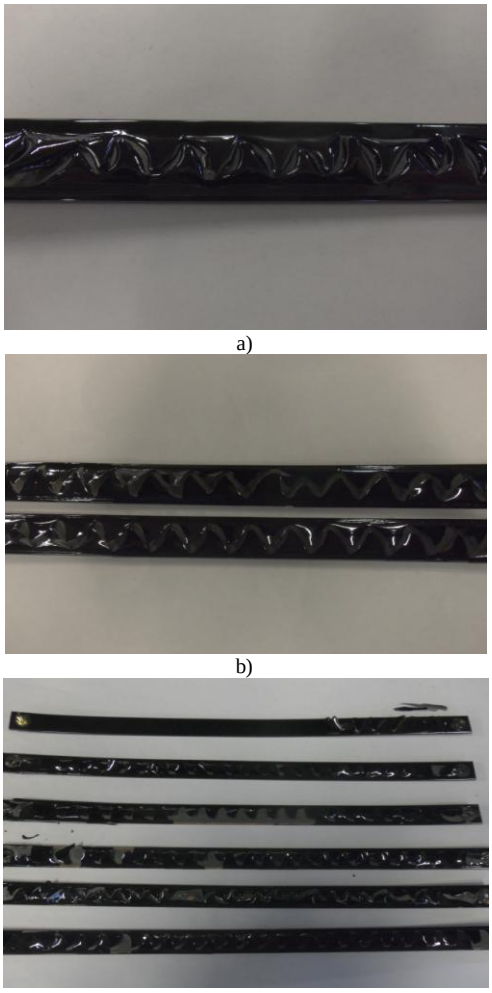

a) b) c)

Fig. 14. Zigzag shaped crack of the insulation material for the samples: a) at 260°C after 400hrs,b) at 245°C after 800hrs and c) at 260°C after 800hrs.

Fig. 15. Aged samples at 275°C after 400hrs.

V. Conclusion

In this work, the polymer insulation coating copper wire for electric motor vehicle winding applications was studied. Dielectric measurements of unaged as well as accelerated aged samples at different temperatures were performed. The results reveal that even unaged insulation samples have manufacturing variations that lead to low capacitance or resistance values. The resistance weak points were found to be less critical than the capacitance ones. Moreover, the aged samples measurements have shown a distinct immediate drop of the insulation capacitance even for light ageing process (200 °C, 100 hrs) which could indicate a change in dielectric permittivity of the material. Furthermore, it is shown that the resistance of the insulation material decreases with increased ageing time up to a critical point when it starts increasing again. This is suspected to be caused by delamination effects, which are permanent material changes in the region between the wire and the insulation material.

References

[1] R. Camilleri, D. A. Howey and M. D. McCulloch, "Thermal Limitations in Air-Cooled Axial Flux In-Wheel Motors for Urban Mobility Vehicles: A preliminary Analysis", Electrical Systems for Aircraft, Railway and Ship Propulsion (ESARS), pp.1-8, Bologna, Italy, Oct. 2012.

[2] H. A. Toliyat, S. Nandi, S. Choi and H. Meshgin-Kelk, "Electric Machines-Modeling, Condition Monitoring and Fault Diagnosis," CRC Press, Taylor & Francis Group, pp. 117-118, 2013.

[3] P. Zhang, Y. Du, T. G. Habetler, and B. Lu, "A survey of condition monitoring and protection methods for medium-voltage induction motors," *IEEE Trans. Ind. Appl.*, vol. 47, no. 1, pp. 34–46, Jan./Feb. 2011.

[4] S. H. Kia, H. Henao and G. Capolino, "Efficient digital signal processing techniques for induction machines fault diagnosis", 2013 IEEE Workshop on Electrical Machines Design Control and Diagnosis (WEMDCD), pp. 232-246, Paris, France, Mar. 2013.

[5] F. Filipetti, A. Bellini and G. Capolino, "Condition monitoring and diagnosis of rotor faults in induction machines: State of the art and future perspectives", 2013 IEEE Workshop on Electrical Machines Design Control and Diagnosis (WEMDCD), pp. 196-209, Paris, France, Mar. 2013.

[6] E. Strangas, S. Aviyente, J. Neely and S. S. H. Zaidi, "Improving the Reliability of Electrical Drives through Failure Prognosis", IEEE 8th SDEMPED, pp. 172-178, Bologna, Italy, Sep. 2011.

[7] R. K. Singleton, E. G. Strangas ans S. Aviyente, "Time-Frequency Complexity Based Remaining Useful Life (RUL) Estimation for Bearing Faults", IEEE 9th SDEMPED, pp. 600-606, Valencia, Spain, Sep. 2013.

[8] A. S. Babel and E. G. Strangas, "Condition-Based Monitoring and Prognostic Health Management of Electric Machine Stator Winding Insulation", IEEE ICEM, pp. 1855-1861, Berlin, Germany, Sep. 2014.

[9] L. Siesing, A. Reinap and M. Andersson, "Thermal properties on high fill factor electrical windings: Infiltrated vs non infiltrated", ICEM, pp. 2218-2223, Berlin, Germany, Sep. 2014.

[10] P. Neti and S. Grubic, "Online Broadband Insulation Spectroscopy of Induction Machines using Signal Injection", IEEE ECCE, pp. 630-637, Pittsburgh, PA, Sep. 2014.

[11] K. Younsi, P. Neti, M. Shah, J. Y. Zhou, J. Krahn and K. Weeber", *IEEE Trans. Diel. Elec. Ins*., Vol. 17, No. 5, pp. 1441-1452, Oct. 2010.

[12] M. Sumislawska, O. Agbaje, D. F. Kavanagh and K. J. Burnham, "Equivalent circuit model estimation of induction machines under elevated temperature conditions", International Conference on Control (UKACC), pp. 413-418, Loughborough, UK, July 2014.

[13] C. Zoeller, M. A. Vogelsberger, P. Nussbaumer and T. M. Wolbank, "Insulation monitoring of three phase inverter-fed ac machines based on two current sensors only," IEEE ICEM, pp. 1901-1907, Berlin, Germany, Sep. 2014.

[14] P. Nussbaumer, M. A. Vogelsberger and T. M. Wolbank, "Induction Machine Insulation Health State Monitoring Based on Online Switching Transient Exploitation," *IEEE Trans. Ind. Elec.*, Vol. 62, No. 3, pp. 1835-1845, Mar. 2015.

[15] N. Lahoud, J. Faucher, D. Malec and P. Maussion, "Electrical Aging of the Insulation of Low-Voltage Machines: Model Definition and Test With the Design of Experiments", *IEEE Trans. Ind. Elec*., Vol. 60, No. 9, pp. 4147-4155, Sep. 2013.

[16] S. Savin, S. Ait-Amar and D. Roger, "Turn-to-Turn Capacitance Variations Correlated to PDIV for AC Motors Monitoring," *IEEE Trans. Diel. Elec. Ins.*, Vol. 20, No. 1, pp. 34-41, Feb. 2013.

[17] Z. Huang, F. J. Marquez-Fernandez, Y. Loayza, A. Reinap and M. Alakula, "Dynamic Thermal Modeling and Application of Electrical Machine in Hybrid Drives", IEEE ICEM, pp. 2158-2164, Berlin, Germany, Sep. 2014.

[18] L. Rux, "The physical phenomena associated with stator winding insulation condition as detected by the ramped direct high-voltage method", Ph.D Thesis Mississipi State University, 2004.

[19] V. Sihvo, "Insulation system in an integrated motor compressor", Ph.D Thesis – Lappeenranta University of Technology, 2010.

[20] G. C. Stone, E. A. Boulter, I. Culbert and H. Dhirani, "Electrical Insulation for Rotating Machines-Design, Evaluation, Aging, Testing and Repair", IEEE Press Series on Power Engineering, 2004.

[21] D. F. Kavanagh, D. A. Howey and M. D. McCulloch, "An Applied Laboratory Characterisation Approach for Electric Machine Insulation", IEEE 9th SDEMPED, pp. 391-395, Valencia, Spain, Sep. 2013.

[22] B. Petitgas, G. Seytre, O. Gain, G. Boiteux, I. Royaud, A. Serghei, A. Gimenez and A. Anton, "High temperature aging of enameled copper wire-relationships between chemical structure and electrical behaviour", Annual Report Conference on Electrical Insulation and Dielectric Phenomena, 2011.

[23] L. Ljung, System Identification: Theory for the User, Prentice Hall, 1999.

Konstantinos N. Gyftakis (M'11**)** was born in Patras, Greece, in May 1984. He received the Diploma in Electrical and Computer Engineering from the University of Patras, Patras, Greece in 2010. He pursued a Ph.D in the same institution in the area of electrical machines condition monitoring and fault diagnosis. Then he worked as a Post-Doctoral Research Assistant in the Dept. of Engineering Science, University of Oxford, UK. He is currently a Lecturer, Faculty of Engineering, Environment and Computing, Coventry University, UK. His research activities are in fault diagnosis, condition monitoring and degradation of electrical machines. He has authored/co-authored more than 30 papers in international scientific journals and conferences. (E-mail: k.n.gyftakis@ieee.org).

Malgorzata Sumislawska received MSc. in Teleinformatics from Wroclaw University of Techlology, Wroclaw Poland (2009) and MSc. in Systems and Control from Coventry University (CU), Coventry, UK (2009). In 2012 she obtained PhD degree in Mathematics and Control Engineering from CU. She is currently a Lecturer in System Identification at CU. Her research includes fault detection and diagnosis, data-based reduced order modeling for control diagnostics and prognostics, state and parameter estimation, and filtering. (Email – malgorzata.sumislawska@coventry.ac.uk)

Darren F. Kavanagh is an Asst. Lecturer at the Institute of Technology Carlow, Ireland. Prior to this he conducted postdoctoral research at the University of Oxford investigating the area of degradation and failure analysis of electric machines with specific applications in electric vehicles. Darren completed his Ph.D. research at Trinity College Dublin in 2011. His doctoral research was in the area of advanced signal processing and pattern recognition for acoustic signals. In 2006, he was awarded an EMBARK scholarship by the Irish Research Council to pursue a Ph.D. on the topic of acoustic signal processing. He was awarded the prestigious Minister's Silver Medal for Science by the Minister for Education (Ireland) in 2004. He has gained valuable academic experience at educational institutions such as, the University of Oxford, Trinity College Dublin and the Institute of Technology Tallaght, ITT Dublin. He has also benefited greatly from industrial experience at Alcatel Lucent-Bell Laboratories, Intel, and Xilinx.

David A. Howey (M'10) received the B.A. and M.Eng. degrees from Cambridge University, Cambridge, U.K., in 2002 and the Ph.D. degree from Imperial College London, London, U.K., in 2010. He is currently an Associate Professor in the Energy and Power Group, Department of Engineering Science, University of Oxford, Oxford, U.K. He leads projects on fast electrochemical modeling, model-based battery management systems, battery thermal management, and motor degradation. His research interests include condition monitoring and management of electric and hybrid vehicle components.

Malcolm D McCulloch (M'89). In 1993 Malcolm moved to Oxford University and to start up the Electrical Power Group (EPG), where is an Associate Professor. The group's focus is to developing, and commercialise, sustainable energy technologies in the four sectors of energy for development, domestic energy use, transport and renewable generation. His work addresses transforming existing power network, designing new power network for the developing world, developing new technology for electric vehicles and developing approaches to integrated mobility. He has over 100 Journal and refereed conference papers, 15 patents and 4 spinout companies.